The protective effect of DNase I in retinal vein occlusion

Guohua Deng [1#], Xi Zou [1#], Zhinan Liu [1#], Hang Ren [2], Yanting Li [3], Bin Chen [3], and Jun Zhang [1*]

Retinal vein occlusion (RVO) ranks as the second most prevalent retinal vascular disease, following diabetic retinopathy. Neutrophil extracellular traps (NETs) play an important role in vascular diseases. This study aimed to elucidate the relationship between NETs and RVO, and to discern the potential role of deoxyribonuclease I (DNase I) in the prevention and treatment of RVO through the modulation of NETs. We analyzed circulating NETs biomarkers, namely, cell-free DNA (cf-DNA), myeloperoxidase (MPO)-DNA, and neutrophil elastase (NE), in 30 RVO patients and 30 healthy individuals. We established an RVO mouse model using a retinal laser, and the mice were categorized into two groups: the DNase I group and the control group. Retinal images were taken at predetermined time points, and the state of the retinal vessels was assessed. Both tissue and blood samples were harvested for analysis of NETs expression through methods, such as western blotting, immunofluorescence staining, and enzyme-linked immunosorbent assay (ELISA). Our findings indicate an increase in circulating NETs biomarkers in human and mouse RVO cases, while also verifying the presence of NETs in the retinal thrombus of the RVO model. Both in vitro and in vivo tests revealed that DNase I attenuated NETs formation. Moreover, DNase I injections led to diminished NETs biomarker levels and a reduced duration of the thrombus after the RVO model establishment. Consequently, DNase I, a well-established modulator of NETs formation, might exhibit protective properties in the prevention and treatment of RVO.

Keywords: Retinal vein occlusion (RVO), neutrophil extracellular traps (NETs), deoxyribonuclease I (DNase I).

Introduction

Retinal vein occlusion (RVO) ranks as the second most common retinal vascular disease, following diabetic retinopathy [1]. Although the development of RVO is widely considered to be associated with vascular thrombosis, oxidative stress, and inflammation, the pathogenesis of RVO still requires further research. Patients diagnosed with RVO may develop vision loss or even blindness when complications, such as neovascular glaucoma and macular edema arise [2]. Currently, RVO complications, including non-perfused areas and neovascular abnormalities, are clinically treated with intravitreal injections of anti-vascular endothelial growth factors, anti-inflammatory glucocorticoids, and retinal laser photocoagulation [3, 4]. Retinal revascularization has undergone extensive research in RVO patients since the injection of a tissue plasminogen activator into the obstructed retinal vein was first reported [5]. However, the complexity of this surgical procedure is hindering its wide applicability in clinical settings.

Neutrophil extracellular traps (NETs) are net-like, extracellular bactericidal structures released by NETosis in response to pathogenic stimuli. They are composed of unwound DNA strands, histones, and bacteriostatic proteins [6]. NETs play a pivotal role in thrombosis pathogenesis, where their net-like structures provide a foundation for red blood cell and platelet aggregation, while their components activate the coagulation pathway [7]. Moreover, in cases of deep vein thrombosis (DVT), inhibiting NETosis has been demonstrated to confer protection [8]. A recent study observed increased NETs-related markers in the peripheral blood of RVO patients, suggesting a potential association between NETs and the development of RVO [9].

Deoxyribonuclease I (DNase I), an economical, convenient, and widely used NETs inhibitor, has rarely been used in the prevention and treatment of RVO. This study aimed to verify the presence of NETs in RVO and assess the protective efficiency of DNase I through in vitro and in vivo experiments, thereby providing a theoretical basis for RVO prevention and treatment.

Materials and methods

Patient selection and parameter testing

We conducted a case-control pilot study, including 30 RVO patients and 30 healthy individuals, between March 2022 and February 2023. The RVO diagnoses were made in accordance with the RVO Preferred Practice Pattern [10]. Following blood sample collection, patients were administered appropriate

[1]Department of Ophthalmology, Changzhou Third People's Hospital, Changzhou Medical Center, Nanjing Medical University, Changzhou, China;   [2]Department of Ophthalmology, The First Affiliated Hospital of Soochow University, Suzhou, China;   [3]Department of Ophthalmology, Suzhou Eye and ENT Hospital, Suzhou, China.

*Correspondence to Jun Zhang: nydczsyzj@163.com

#Guohua Deng, Xi Zou, and Zhinan Liu contributed equally to this work.

treatments. Participants were excluded from the study if they met any of the following criteria: (1) a history of thrombotic disorders or systemic inflammation; (2) a history of uveitis or iris rubeosis; (3) previous RVO treatment history; (4) hematological or connective tissue disorders, malignant tumors, or an inability to cooperate with the study's requirements.

The coagulation function parameters, including activated partial thromboplastin time (APTT), fibrinogen (FIB), thrombin time (TT), and prothrombin time (PT), were assessed using an automatic coagulation function analyzer (SYSMEX, CA-1500), and the serum levels of myeloperoxidase (MPO) and neutrophil elastase (NE) were measured using commercially available enzyme-linked immunosorbent assay (ELISA) kits (MULTI SCIENCES, China; Abcam, USA). The cell-free DNA (cf-DNA) was measured using a method similar to ELISA. In brief, a standard calf thymus solution (Sigma-Aldrich, Germany) was prepared in a concentration gradient. A volume of 100 μL each of serum and calf thymus solution was added to 96-well plates. After a reaction period of 30 min with 100 μL of SYTOX green (ThermoFisher Scientific, USA), the fluorescence intensity was measured at 485 nm, from which the concentration of cf-DNA was calculated.

In vitro experiment
Neutrophils were extracted from healthy volunteers using a neutrophil isolation kit (Beijing Solarbio Science & Technology, China). The cells were seeded onto a 12-well plate at a density of 1.5×10^6 cells/well and were then equally divided into three groups. As described in previous studies, the DNase I group was treated with 100 U/mL DNase I (Beijing Solarbio Science & Technology, China) and 20 nM phorbol-12-myristate-13-acetate (PMA) [11]. The PMA group was treated solely with 20 nM PMA, while the remaining wells received Roswell Park Memorial Institute 1640 (RPMI 1640) medium stimulation. After a 4 h incubation, all groups underwent SYTOX green staining for 30 min. Subsequently, slides were photographed under an inverted fluorescence microscope (Leica DMILLED, Leica, Germany) and the cf-DNA levels in the culture medium were measured as previously described.

Animal experiments
C57 mice were procured from JOINN Laboratories (Suzhou, China). Twenty eight-week-old male mice were randomly divided into RVO and control groups, with each group consisting of ten mice. NETs-related biomarkers were analyzed to confirm the differences between RVO and healthy groups. The RVO model was established as described below. Mice in the control group were exposed to an equal-energy laser between retinal vessels to account for any non-specific laser-induced damage. Following the establishment of the RVO model, serum MPO, NE, and cf-DNA levels were measured in both groups. In a separate setup, 74 eight-week-old male mice were randomly divided into DNase I and control groups, with each group consisting of 37 mice. Twelve mice were selected at random from each group for retinal imaging, while the remaining mice were set aside for sample collection at the different subsequent time

points, as described below. The DNase I dosage was based on previous research. To elaborate, the DNase I group was administered an intravenous injection of 50 U/mouse DNase I both 1 h before and 24 h after the RVO model establishment. In contrast, the control group was injected with an equivalent volume of phosphate-buffered saline (PBS) [12].

Retinal vein occlusion model establishment
After pupil dilation, the mice were administered an injection of 37.5 mg/kg Rose Bengal (Sigma-Aldrich, Germany) via the tail vein. Following anesthesia, the two thick retinal veins were irradiated with a 532 nm fundus laser (VISULAS 532 s, Carl Zeiss, Germany). The used laser parameters were: 100 mW laser power, 50 μm spot size, a distance of 375 μm from the spot to the optic disc, 100 μm spot spacing, 1000 ms single spot time, 1000 ms exposure duration, and three laser spots per vein.

Image acquisition
Fundus images were acquired prior to laser therapy and at subsequent intervals of 4 h, 1 d, 3 d, and 8 d after establishing the RVO model. Three independent investigators analyzed the images to assess vessel obstruction. In instances of differing opinions, a vessel was deemed obstructed if at least two of the three investigators considered it so, otherwise, it was recorded as unobstructed. The images were acquired using the anterior segment imaging system, with a coverslip coated with ophthalmic gel placed in front of the eye under examination.

Sample collection and storage
A certain volume of blood was drawn from the heart 0.5 h before and 4 h, 1 d, 3 d, and 8 d after the RVO model establishment. At each of these time points, five mice were randomly selected from each group for blood collection. For the serum samples, portions of the blood (500 μL) were transferred to 1.5 mL centrifuge tubes without anticoagulants. These samples were then allowed to rest for 60 min before being centrifuged at 3000 rpm for 10 min at 4 °C. Subsequently, the supernatant was collected and stored in centrifuge tubes at −80 °C.

In a preliminary experiment, NETs biomarkers peaked 24 h after laser therapy. As a result, eye samples were collected for histological evaluation at this time, along with the retinal protein extraction conducted at this time for western blotting analysis.

Neutrophil extracellular traps biomarker monitoring
The concentrations of MPO-DNA complexes and NE in mice's peripheral blood were assessed using an ELISA kit (MEIMIAN, China; Abcam, USA). Serum cf-DNA levels were determined after reacting with SYTOX green (ThermoFisher Scientific, USA) by comparing its absorbance to that of standard calf thymus (Sigma, USA). Additionally, a western blot of retinal proteins was conducted to analyze the citrullinated histone H3 (H3cit) and MPO (Abcam, USA).

Ethical statement
All study procedures adhered to the Association for Research in Vision and Ophthalmology Statement for the Use of Animals in Ophthalmic and Vision Research. Furthermore, all study

Table 1. Clinical characteristics and laboratory data of RVO cases and healthy controls

	Control group	RVO group	P value
Sex (male)	50%	52%	0.796
Age (years)	61.6 ± 4.5	60.7 ± 3.9	0.466
Diabetes	10 (33.0%)	13 (43.3%)	0.426
Hypertension	14 (47.0%)	12 (40.0%)	0.602
Smoking	7 (23.3%)	13 (43.3%)	0.100
Drinking	6 (20.0%)	11 (36.6%)	0.152
PT (s)	12.4 ± 1.0	10.9 ± 1.4	< 0.001
APTT (s)	33.2 ± 3.2	31.4 ± 1.9	0.013
TT (s)	15.6 ± 1.4	15.5 ± 1.3	0.726
FIB (g/L)	3.1 ± 0.4	4.1 ± 0.9	< 0.001

Data are presented as n (%) or mean ± standard deviation. Comparison between groups was calculated using the unpaired t-test and chi-square exact test. RVO: Retinal vein occlusion; PT: Prothrombin time; APTT: Activated partial thromboplastin time; TT: Thrombin time; FIB: Fibrinogen.

operations were conducted in accordance with the World Medical Association Declaration of Helsinki. The study protocol received approval from the Ethics Committee of Changzhou Third People's Hospital (02A-A20210014). The clinical experiment was registered in the Chinese Clinical Trial Registry (ChiCTR2200056618). Written informed consent was obtained from all participants involved in this study.

Statistical analysis
Images from immunofluorescence were analyzed using ImageJ. Statistical analyses were performed using Origin 2021 and SPSS 24.0. Continuous data were presented as mean ± standard deviation (SD). The differences between the two groups were analyzed using a non-paired t-test and a chi-squared test. A P value of < 0.05 was considered statistically significant.

Results
Participants' characteristics
A total of 30 RVO patients and 30 healthy controls were included in this research. There were no significant differences in age, sex, presence of hypertension, diabetes, smoking, and drinking habits between the groups (P > 0.05). The indices of thrombotic function were increased in the RVO group (P < 0.05). The clinical characteristics and laboratory indices for both groups are presented in Table 1.

Increased neutrophil extracellular traps biomarkers in retinal vein occlusion
To ascertain the relationship between NETs biomarkers and RVO incidences, circulating NETs remnants, including cf-DNA, MPO-DNA, and NE concentrations were measured in both humans and the RVO mouse model. In comparison to the control group (healthy people), levels of cf-DNA, MPO-DNA, and NE

were increased to 40.8 ± 12.8 ng/mL, 528.4 ± 154.3 ng/mL, and 6.6 ± 2.4 ng/mL, respectively (Figure 1A–1C). In the RVO model, circulating NETs remnants of cf-DNA, MPO-DNA, and NE were 74.8 ± 19.3 ng/mL, 124.8 ± 23.1 ng/mL, and 40.3 ± 17.3 ng/mL, respectively, showing a significant increase compared to the control group (Figure 1D–1F).

### Effect of DNase I on neutrophil extracellular traps in in vitro experiments
Neutrophils were extracted, stimulated, and stained as previously described. Cells were stimulated with 20-nM PMA to induce NETs formation and DNase I (100 U/mL) was introduced to attenuate this induction (Figure 2A). Immunofluorescence images were captured at different magnifications. Five images at 10× magnification were randomly selected from each group for analysis using ImageJ. Significant differences in the area of NETs fluorescent staining were observed among the control, PMA, and DNase I groups (Figure 2B). The culture medium cf-DNA levels of the control, PMA, and PMA + DNase I groups were 93 ± 4.7 ng/mL, 341.4 ± 42.5 ng/mL, and 183.5 ± 14.6 ng/mL, respectively (Figure 2C).

DNase I inhibits neutrophil extracellular traps formation in retinal vein occlusion mouse model
After the retinal laser therapy, the cf-DNA, MPO-DNA, and NE concentrations increased in the mice's peripheral blood. The NETs biomarkers in the RVO + DNase I group were notably lower than those in the RVO group (Figure 3A–3C). The peak levels of circulating NETs biomarkers were observed on the first day following the model establishment, and consequently, retinal proteins and eyeballs were collected for western blot analysis and fluorescent immunostaining. The expression of NETs-related markers, including MPO and H3cit, within the retinal thrombus, were lower after the DNase I injection (Figure 3D–3F). Western blot analysis revealed an increase in MPO and H3cit levels after the retinal laser procedure, which was counteracted by DNase I, suppressing this increase (Figure 3G–3I).

DNase I shortens the duration of the thrombus existence in retinal vein occlusion
In mice subjected to retinal laser therapy, fundus images were acquired before the treatment and at intervals of 4 h, 1 d, 3 d, and 8 d after the treatment. In the RVO model, observations included vessels that were not occluded, completely occluded vessels, patchy bleeding, and reperfusion subsequent to occlusion (Figure 4A). The state of the occlusion changed within the first 10 min after retinal laser therapy and remained stable during the first 24 h [13]. Consistent with previous research, most occlusions experienced reperfusion by the eighth day after irradiation [14], and our findings indicate that DNase I accelerated the reperfusion (Figure 4B). Moreover, the average duration of the retinal thrombus in the RVO + DNase I group was 1.85 ± 2.23 days, which was less than that observed in the RVO group (Figure 4C).
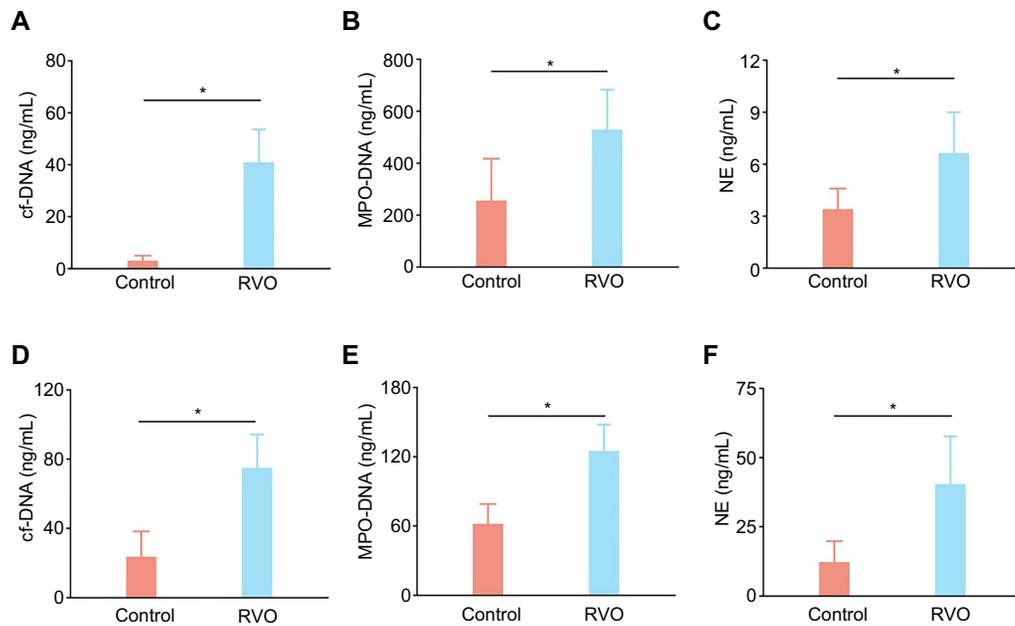
Figure 1. Comparative levels of NETs biomarkers in RVO cases vs healthy controls. (A–C) Levels of NETs biomarkers measured in human RVO cases and healthy controls. Circulating NETs biomarkers (cf-DNA [A], MPO-DNA [B], and NE [C]) were higher in RVO patients compared to the controls ($n = 30$ per group; $*P < 0.05$). (D–F) Levels of NETs biomarkers measured in mice RVO model group and healthy controls group. Circulating NETs biomarkers (cf-DNA [D], MPO-DNA [E], and NE [F]) were higher in the RVO model group compared to the control group ($n = 10$ per group; $*P < 0.05$). NETs: Neutrophil extracellular traps; RVO: Retinal vein occlusion; cf-DNA: Cell-free DNA; MPO: Myeloperoxidase; NE: Neutrophil elastase.
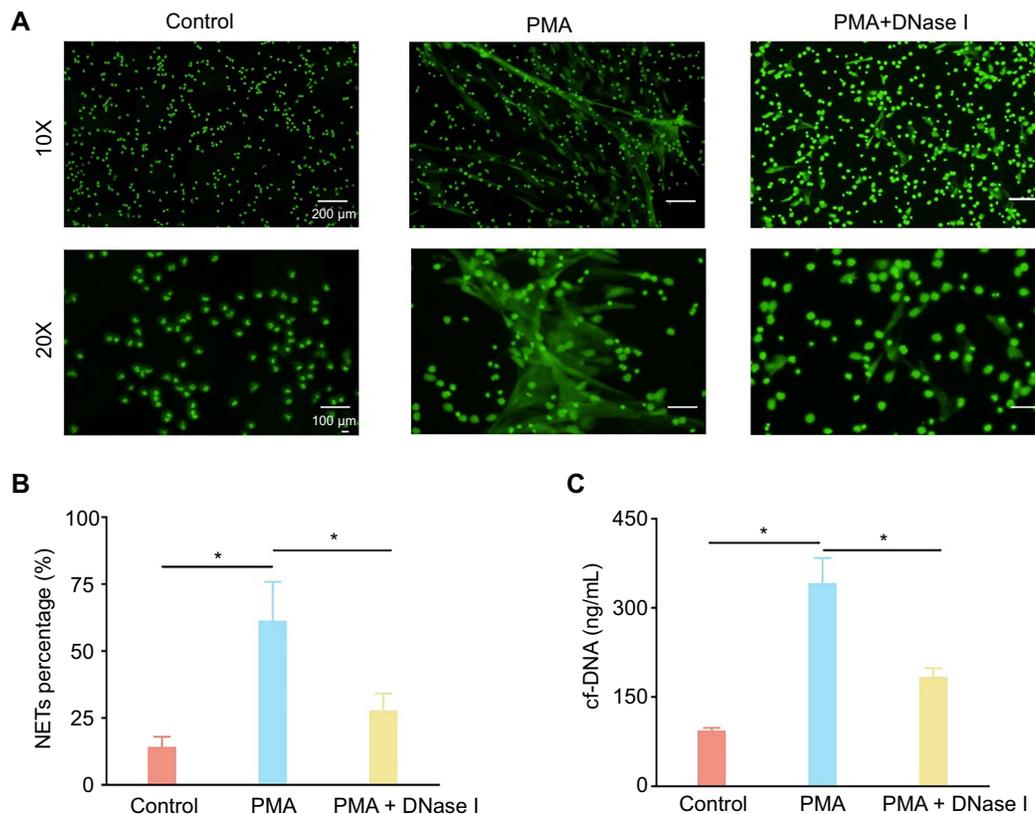
Figure 2. DNase I attenuates NETs formation in vitro. In the control group, the neutrophils were treated with RPMI 1640 for 4 h. In the PMA group, the neutrophils were stimulated with 20 nM PMA for a duration of 4 h. For the PMA + DNase I group, the neutrophils were treated with DNase I (100 U/mL) for 0.5 h before being exposed to PMA. (A) Immunofluorescence images of neutrophils under different conditions: control, PMA-stimulated, and PMA + DNase I-treated groups, with both $10\times$ and $20\times$ magnifications; (B) Quantitative analysis showcasing the percentage of NETs formation across the different groups ($n = 5$; $*P < 0.05$); (C) Bar graph illustrating the levels of cf-DNA in the culture medium across the different groups ($n = 3$; $*P < 0.05$). DNase I: Deoxyribonuclease I; RPMI 1640: Roswell Park Memorial Institute 1640 medium; PMA: Phorbol-12-myristate-13-acetate; NETs: Neutrophil extra-cellular traps; cf-DNA: Cell-free DNA.

Deng et al.
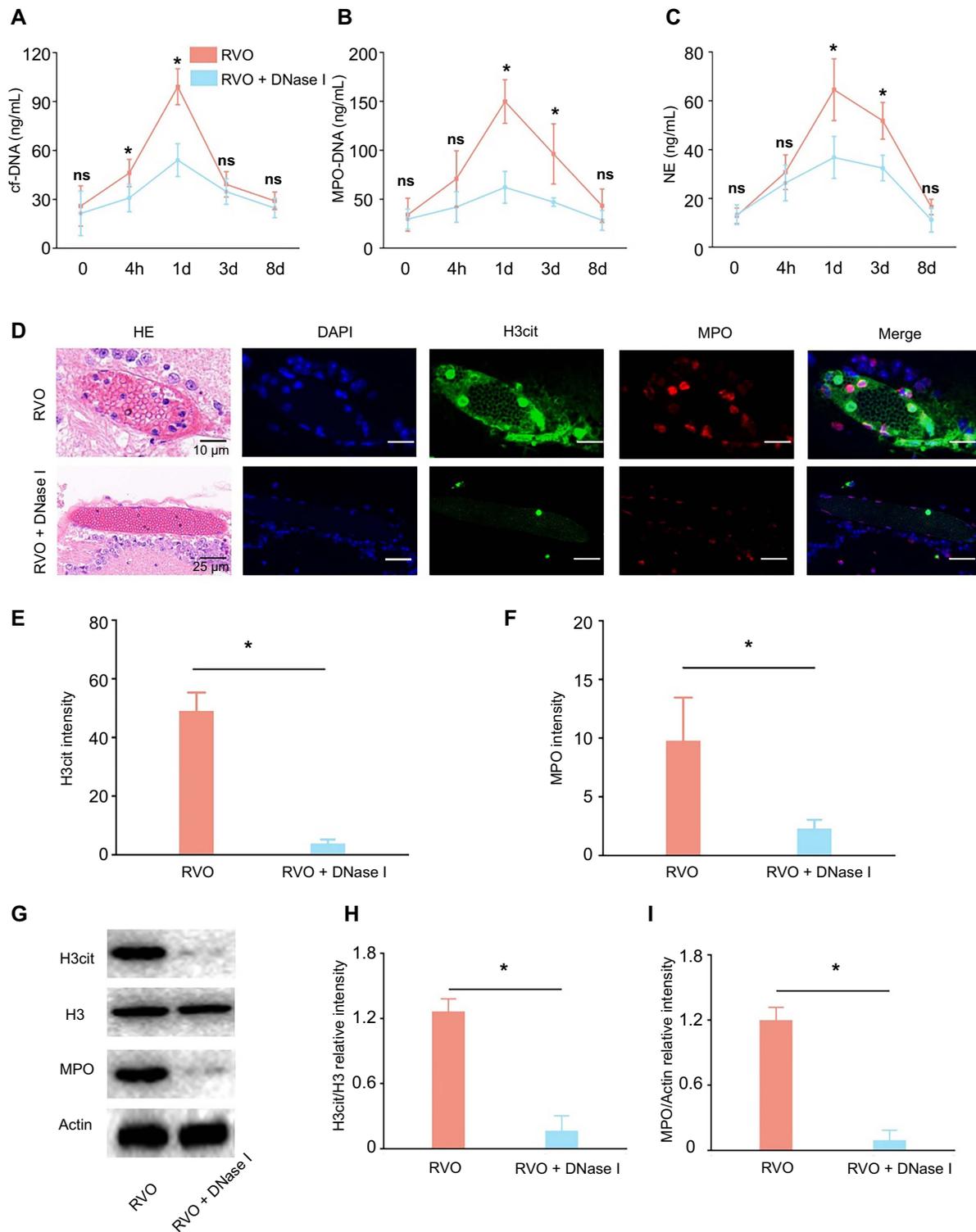
Figure 3. DNase I attenuates NETs formation in vivo. (A–C) Time-course graphs depicting the changes in circulating NETs biomarkers, cf-DNA(A), MPO-DNA (B), and NE (C), following retinal laser therapy, with the RVO + DNase I group showing diminished levels in comparison to the RVO group ($n = 3$; *$P < 0.05$). (D) Histological and immunohistological images showing decreased MPO and H3cit expression in RVO thrombus after the DNase I injection. (E and F) Semi-quantitative analysis of H3cit (E) and MPO (F) immunofluorescence intensity in both the RVO and RVO + DNase I groups ($n = 3$; *$P < 0.05$). (G) Western blot analysis of the H3cit and MPO relative protein expression in the retinas of both the RVO and RVO + DNase I groups. (H and I) Semi-quantitative analysis of the H3cit (H) and MPO (I) protein expression in both the RVO and RVO + DNase I groups ($n = 3$; *$P < 0.05$). DNase I: Deoxyribonuclease I; NETs: Neutrophil extracellular traps; cf-DNA: Cell-free DNA; MPO: Myeloperoxidase; NE: Neutrophil elastase; RVO: Retinal vein occlusion; H3cit: Citrullinated histone H3; ns: Non-significant; HE: Hematoxylin and eosin; DAPI: 4′,6-diamidino-2-phenylindole; H3: Histone 3.
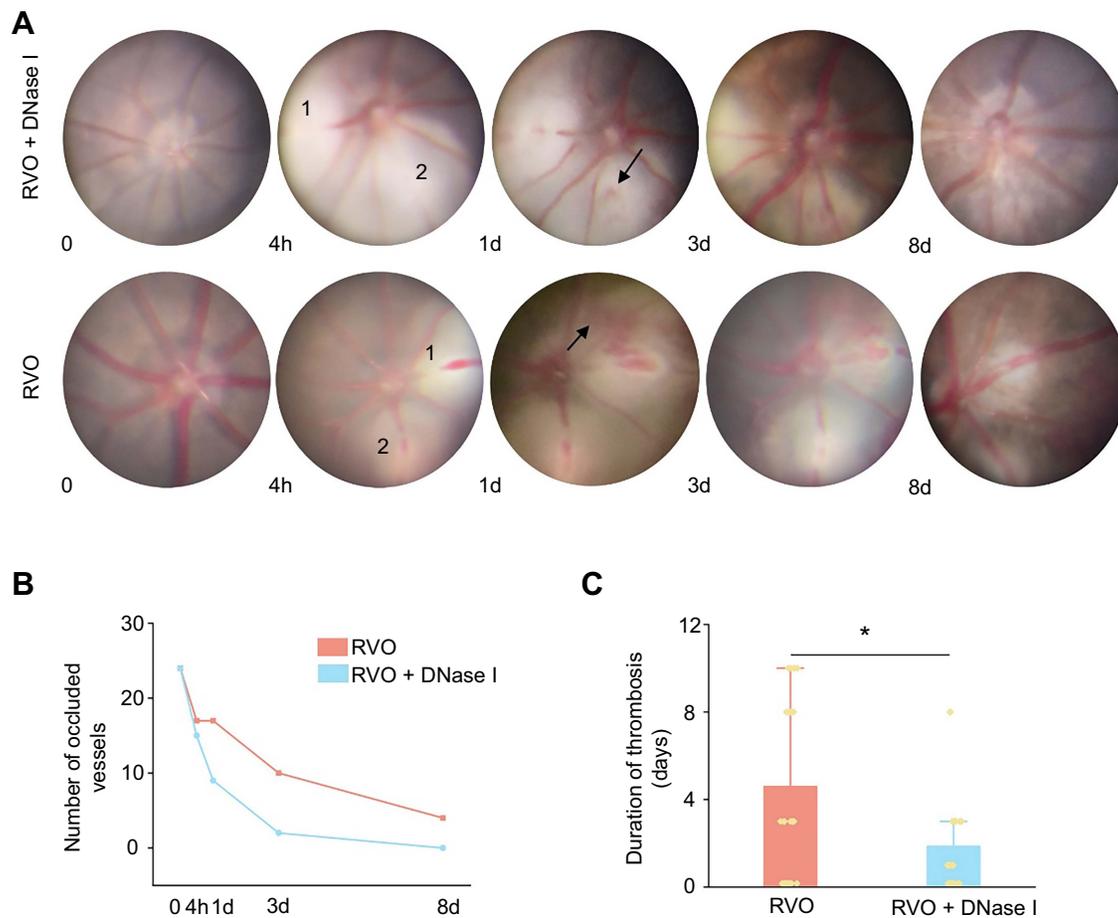
Figure 4. **DNase I shortens the duration of the RVO thrombus**. (A) Representative retinal pictures of RVO and RVO + DNase I groups taken at different time intervals post-laser treatment, with "0" indicating before laser treatment. Veins labeled as "1" and "2" are the ones that received laser irradiation, and retinal bleeding can be observed (indicated by an arrowhead); (B) Graph depicting the number of occluded retinal vessels over time for both groups; (C) Duration of thrombus presence in retinal vessels for both RVO and RVO + DNase I groups ($n = 24$; $*P < 0.05$). DNase I: Deoxyribonuclease I; RVO: Retinal vein occlusion.

Discussion

As a common retinal vascular disease, RVO is prone to causing visual impairment and even blindness due to complications. While many studies have focused on the treatment and complications of RVO, and factors like inflammation and oxidative stress are believed to be associated with RVO, the detailed mechanisms are not fully understood [15]. NETs are net-like DNA structures released by neutrophils through the NETosis mechanism, containing MPO, H3cit, NE, and DNA as their components [9, 16]. Moreover, MPO-DNA, cf-DNA, and NE, widely utilized as NETs-related markers [17, 18], were selected to assess the NETs levels in the peripheral blood. Meanwhile, MPO and H3cit were analyzed using western blot and immunofluorescence techniques. Previous studies have shown that NETs can stimulate intrinsic and extrinsic coagulation pathways [19], leading to platelet activation, adhesion, and aggregation, while the interaction between NETs and platelets can lead to a vicious cycle of NETs formation and platelet activation [20]. Additionally, NETs can recruit red blood cells, promote fibrin deposition, induce thrombosis, and enhance the stability of the venous thrombus [19]. Recently, elevated levels of NETs-related markers were found in the peripheral blood of RVO patients [9], a finding that is consistent with our clinical experiment results. In addition, NETs might promote numerous coagulant factors and thrombosis [21, 22], therefore, we evaluated the thrombotic function indices and found that the average FIB level in RVO patients exceeded the normal range, suggesting a potential association with the NETs status.

The exact role of NETs in RVO still necessitates powerful and direct evidence, including analyses of retinal tissues. Pondering whether inhibiting NETs might shorten the duration of retinal thrombus and alleviate RVO symptoms, our team developed an RVO mouse model for further research.

During our animal experiments, after the establishment of the RVO model, circulating NETs levels increased on day 1, with a subsequent decrease over the following days. This pattern might have been related to the thrombus stability within the first 24 h [13], and the continuous production of NETs. As the days passed and the occluded vessels began to recanalize, circulating NETs levels decreased. A German study

Deng et al.
DNase I inhibits retinal vein occlusion
392
www.biomolbiomed.com

detected the presence of NETs in DVT, and demonstrated that DNase-I could curb DVT progression by limiting NETs [8]. In our research, DNase I effectively decreased NETs expression both in the retina and peripheral blood. Notably, the difference in NETs reduction appeared more pronounced in the retina, possibly due to its inherently low baseline expression of NETs-related biomarkers. Furthermore, utilizing DNase I resulted in a reduced duration of retinal thrombosis compared to the control group. These findings indicate that NETs could play an important role in RVO and that DNase I might emerge as a novel preventive and therapeutic option for RVO. Nonetheless, although NETs are known to initiate and propagate venous thrombosis and promote fibrous vascular occlusion in chronic thrombosis [8, 23], their specific role in RVO demands further in-depth research. Interestingly, our data revealed that the number of smokers in the RVO group was nearly double that of the control group, offering another intriguing avenue for future research.

This study had some limitations that future research should address. Firstly, while the finding indicates an association between the NETs and RVO development and suggests a beneficial role for DNase I in the treatment of RVO, the relationship between different DNase I doses and in vivo NETs levels needs exploration to determine the most effective dose for RVO prevention or treatment. Secondly, due to the unavailability of certain tools, some RVO-related assessments, such as optical coherence tomography (OCT), were not conducted in the RVO model. Incorporating larger sample sizes and utilizing DNase I knocked out (KO) mice could enhance the robustness of the evidence. Lastly, a deeper understanding of the exact pathways and mechanisms through which DNase I treats RVO is still necessary.

Conclusion

In conclusion, the plasma NETs remnants were found to be significantly increased in RVO patients. In our animal experiments, upon successful establishment of the RVO model, NETs biomarkers showed a significant increase. With the injection of DNase I, NETs formation was inhibited, making the thrombus more unstable. This indicates a potential new target for RVO treatment. Further studies and clinical trials are necessary to identify the exact mechanism by which DNase I, in inhibiting NETs, may aid in the prevention and treatment of RVO.

Acknowledgements

We extend our gratitude to Dr. Xi Kun and Dr. Jincheng Tang for providing guidelines for in vitro experiments.

References

[1] Freund KB, Sarraf D, Leong BCS, Garrity ST, Vupparaboina KK, Dansingani KK. Association of optical coherence tomography angiography of collaterals in retinal vein occlusion with major venous outflow through the deep vascular complex. JAMA Ophthalmol 2018 Nov 1;136(11):1262–70. https://doi.org/10.1001/jamaophthalmol.2018.3586.

[2] Rong AJ, Swaminathan SS, Vanner EA, Parrish RK, II. Predictors of neovascular glaucoma in central retinal vein occlusion. Am J Ophthalmol 2019 Aug;204:62–9. https://doi.org/10.1016/j.ajo.2019.02.038.

[3] Hayreh SS. Photocoagulation for retinal vein occlusion. Prog Retin Eye Res 2021 Nov;85:100964. https://doi.org/10.1016/j.preteyeres.2021.100964.

[4] Pham B, Thomas SM, Lillie E, Lee T, Hamid J, Richter T, et al. Anti-vascular endothelial growth factor treatment for retinal conditions: a systematic review and meta-analysis 2019 May 28;9(5):e022031. https://doi.org/10.1136/bmjopen-2018-022031.

[5] Weiss JN. Treatment of central retinal vein occlusion by injection of tissue plasminogen activator into a retinal vein. Am J Ophthalmol 1998 Jul;126(1):142–4. https://doi.org/10.1016/S0002-9394(98)00086-5.

[6] Laridan E, Martinod K, De Meyer SF. Neutrophil extracellular traps in arterial and venous thrombosis. Semin Thromb Hemost 2019 Feb;45(1):86–93. https://doi.org/10.1055/s-0038-1677040.

[7] Noubouossie DF, Reeves BN, Strahl BD, Key NS. Neutrophils: back in the thrombosis spotlight. Blood 2019;133(20):2186–97. https://doi.org/10.1182/blood-2018-10-862243.

[8] von Brühl M-L, Stark K, Steinhart A, Chandraratne S, Konrad I, Lorenz M, et al. Monocytes, neutrophils, and platelets cooperate to initiate and propagate venous thrombosis in mice in vivo. J Exp Med 2012;209(4):819–35. https://doi.org/10.1084/jem.20112322.

[9] Wan W, Liu H, Long Y, Wan W, Li Q, Zhu W, et al. The association between circulating neutrophil extracellular trap related biomarkers and retinal vein occlusion incidence: a case-control pilot study. Exp Eye Res 2021 Sep;210:108702. https://doi.org/10.1016/j.exer.2021.108702.

[10] Flaxel CJ, Adelman RA, Bailey ST, Fawzi A, Lim JI, Vemulakonda GA, et al. Retinal vein occlusions preferred practice pattern®. Ophthalmol 2020 Feb;127(2):P288–320. https://doi.org/10.1016/j.ophtha.2019.09.029.

[11] Yang LY, Luo Q, Lu L, Zhu WW, Sun HT, Wei R, et al. Increased neutrophil extracellular traps promote metastasis potential of hepatocellular carcinoma via provoking tumorous inflammatory response. J Hematol Oncol 2020 Jan 6;13(1):3. https://doi.org/10.1186/s13045-019-0836-0.

[12] Hisada Y, Grover SP, Maqsood A, Houston R, Ay C, Noubouossie DF, et al. Neutrophils and neutrophil extracellular traps enhance venous thrombosis in mice bearing human pancreatic tumors. Haematologica 2020 Jan;105(1):218–25. https://doi.org/10.3324/haematol.2019.217083.

[13] Colón Ortiz C, Potenski A, Lawson JM, Smart J, Troy CM. Optimization of the retinal vein occlusion mouse model to limit variability. J Vis Exp 2021 Aug;6(174):10.3791/62980. https://doi.org/10.3791/62980-v.

[14] Avrutsky MI, Ortiz CC. Endothelial activation of caspase-9 promotes neurovascular injury in retinal vein occlusion. Nat Commun 2020 Jun 23;11(1):3173. https://doi.org/10.1038/s41467-020-16902-5.

[15] Rehak M, Wiedemann P. Retinal vein thrombosis: pathogenesis and management. J Thromb Haemost 2010 Sep;8(9):1886–94. https://doi.org/10.1111/j.1538-7836.2010.03909.x.

Deng et al.
DNase I inhibits retinal vein occlusion
393
www.biomolbiomed.com

[16] Fuchs TA, Abed U, Goosmann C, Hurwitz R, Schulze I, Wahn V, et al. Novel cell death program leads to neutrophil extracellular traps. J Cell Biol 2007 Jan 15;176(2):231–41. https://doi.org/10.1083/jcb.200606027.

[17] Middleton EA, He XY, Denorme F, Campbell RA, Ng D, Salvatore SP, et al. Neutrophil extracellular traps contribute to immunothrombosis in COVID-19 acute respiratory distress syndrome. Blood 2020 Sep 3;136(10):1169–79. https://doi.org/10.1182/blood.2020007008.

[18] Zuo Y, Yalavarthi S, Shi H, Gockman K, Zuo M, Madison JA, et al. Neutrophil extracellular traps in COVID-19. JCI Insight 2020 Jun 4;5(11):e138999. https://doi.org/10.1172/jci.insight.138999.

[19] Fuchs TA, Brill A, Duerschmied D, Schatzberg D, Monestier M, Myers DD, et al. Extracellular DNA traps promote thrombosis. Proc Nat Acad Sci USA 2010 Sep 7;107(36):15880–5. https://doi.org/10.1073/pnas.1005743107.

[20] Watson K, Gooderham NJ, Davies DS, Edwards RJ. Nucleosomes bind to cell surface proteoglycans. J Biol Chem 1999 Jul 30;274(31):21707–13. https://doi.org/10.1074/jbc.274.31.21707.

[21] Zhou P, Li T, Jin J, Liu Y, Li B, Sun Q, et al. Interactions between neutrophil extracellular traps and activated platelets enhance procoagulant activity in acute stroke patients with ICA occlusion. EBioMed 2020 Mar;53:102671. https://doi.org/10.1016/j.ebiom.2020.102671.

[22] Dhanesha N, Nayak MK, Doddapattar P, Jain M, Flora GD, Kon S, et al. Targeting myeloid-cell specific integrin $\alpha 9\beta 1$ inhibits arterial thrombosis in mice. Blood 2020 Mar 12;135(11):857–61. https://doi.org/10.1182/blood.2019002846.

[23] Sharma S, Hofbauer TM, Ondracek AS, Chausheva S, Alimohammadi A, Artner T, et al. Neutrophil extracellular traps promote fibrous vascular occlusions in chronic thrombosis. Blood 2021 Feb 25;137(8):1104–16. https://doi.org/10.1182/blood.2020005861.

Related articles published in BJBMS

1. Efficacy and safety of PEG-rhG-CSF in preventing chemoradiotherapy-induced neutropenia in patients with locally advanced cervical cancer

   Weiwei Li et al., Biomol Biomed, 2023